Deadbeat Predictive Current Control for PMSM

NIU Li ,YANG Ming, XU Dian-guo
Institute of Power Electronics and Electrical Drives
Harbin Institute of Technology, Harbin 150080, China
e-mail: yangming@hit.edu.cn

Abstract—**In this paper a predictive current control for PMSM based on dead-beat algorithm is proposed, in the synchronous rotary frame, to improve the performance of current loop. Based on the mathematical model of PMSM the current controller calculated the expected voltage vector directly in terms of the current reference and feedback values, after that transforms the voltage vector into switch signals with SVPWM model. The robust predictive current control is introduced to decrease the sensitivity of system stability with the model parameters error. Simulation and experiment results show that the PMSM predictive current control scheme improves both the dynamic performance and steady-state precision of the current loop efficiently.**

Keywords- permanent magnet synchronous motor; current control; predictive control; robustness

I. INTRODUCTION

Due to the inherent characteristic of servo system, i.e. the control structure contain 3 loops, the bandwidth of current loop which is the inner loop of the 3 control loops, is critical factor that influence the dynamic performance of servo system. The target of current loop control is to force the current feedback following the current reference, and make the control system has excellent dynamic and stabilization performance. At present, field oriented control (FOC) is applied into most AC servo system, the controllers using PI regulators to control quadrature and direct axis currents in the synchronous rotating frame, that means the motor currents which are alternative variables can be controlled as DC variables, thereby it will simplify the control process and enhance the control accuracy[1-3]. Along with the development of integrated circuit technology, numerical control (NC) system is extensively applied in the servo system for its advantages of compact size, low cost, and the immunity from interference[4-7]. However, as a result of inherent characteristic of keeping and quantization links in numerical control system, the servo system is controlled periodically, that adopts a lots of delay links into the control system, such as delays of current sampling, PWM duty-cycle updating, inverter outputting, inverter's dead-zone and all kinds of filtering links[8]. It results in that the controller outputs lag behind the variation of system current. So that, in order to improve the system performance, it has to make the control period as short as possible. If the time consumption of control algorithm is constant, the control algorithm shares more proportion of system control period when the control period gets shorter, therefore the shorter control period will restrict the system software resource. The dual sampling and dual updating strategy that proposed in [8] is to sample motor current 2 times in the mean time calculate and update duty-cycle, thus reduces a half of the system delay and improves the current loop performance. However this current loop strategy needs a lot of software resource to calculate double control code, and it can not reduce the system delay further with a fixed PWM frequency, hence the current loop is not optimal.

Compared with traditional FOC, predictive control will result in better dynamic performance and less current harmonics. Predictive control can be categorized in 3 kinds with different vector combination method. [10-11] proposes a method that predicts the motor current of next control period based on the 7 different voltage vectors which are the output of inverter, then using a cost function to specify the output voltage vector from the 7 vectors. It brings high bandwidth current loop with significant current ripple. [12-13] gives a method that select a nonzero voltage vector on the basis of present system state and spacial section, then combination this nonzero vector with zero vector to minimize the difference between the predictive and reference current value during the next interval. [14-17] calculates the expect voltage which force the motor current equal to the current reference based on the predictive function, then translate the voltage signal into switch signals with PWM technology. The expect voltage is the combination of 2 nonzero voltage vectors and zero voltage vectors, it is same with traditional FOC, so that better current dynamic and smaller current ripple can be got from this method. The last method is known as PPC in [16], sometimes called dead-beat control, and is noted as deadbeat predictive control in this paper.

This paper proposes a deadbeat predictive control in the synchronous rotating frame on the basis of PMSM mathematical model. In order to overcome the instability due to parameter inaccuracy, a robust current control algorithm is adopted. Theoretically, this algorithm makes the motor current reach its reference within 2 control period. Experimental platform is based on TMS320F2812 DSP. Simulation and experiment results show that the PMSM current predictive control scheme improves both the dynamic performance and steady-state precision of the current loop efficiently.

II. ESTABLISHING OF SYSTEM MODELSE

A. PMSM Mathmatical Model

The voltage equations of PMSM in synchronous rotating frame is shown as follows,

$$u_d = Ri_d + \frac{d\psi_d}{dt} - \psi_q \omega_e \tag{1}$$

Supported by National Natural Science Foundation of China (51007012)

$$u_q = Ri_q + \frac{d\psi_q}{dt} + \psi_d \omega_e \tag{2}$$

Where, $\psi_d = L_d i_d + \psi_f$ is direct axis flux. $\psi_q = L_q i_q$ is quadrature axis flux. u_d, u_q, i_d, i_q is direct and quadrature axis voltages and currents respectively. ω_e is electrical angular velocity. ψ_f, R, L_d, L_q is permanent magnet flux, stator resistance, direct and quadrature axis inductance respectively.

Based on the voltage equations, letting the motor currents as state variables, if the PMSM is surface mounted motor and $L_d = L_q = L$, then the following state space function can be got,

$$\begin{bmatrix} \frac{di_d}{dt} \\ \frac{di_q}{dt} \end{bmatrix} = \begin{bmatrix} -\frac{R}{L} & \omega_e \\ -\omega_e & -\frac{R}{L} \end{bmatrix} \begin{bmatrix} i_d \\ i_q \end{bmatrix} + \begin{bmatrix} \frac{1}{L} & 0 \\ 0 & \frac{1}{L} \end{bmatrix} \begin{bmatrix} u_d \\ u_q \end{bmatrix} + \begin{bmatrix} 0 \\ -\frac{\psi_f}{L}\omega_e \end{bmatrix} \tag{3}$$

Letting the motor currents as state variables, according the structure of standard state space function, (3) can be re-written as $\dot{\boldsymbol{x}} = \boldsymbol{Ax} + \boldsymbol{Bu} + \boldsymbol{d}$, and the continuous general solution of the state space function is shown as follows,

$$\boldsymbol{x}(t) = e^{\boldsymbol{A}(t-t_0)}\boldsymbol{x}(t_0) + \int_{t_0}^{t} e^{\boldsymbol{A}(t-\tau)}(\boldsymbol{Bu}(\tau) + \boldsymbol{d}(\tau))d\tau \tag{4}$$

In order to get the discrete current state equation, regarding the system input u is constant during kT~$(k+1)T$ interval when sampling period T is small enough. Variable d represents the influence of back EMF, it can also be regarded as constant during the sampling period, because d is a low time varying variable compared with motor currents. Then letting $t_0=kT$ and $t=(k+1)T$, and the following equation is the discrete general solution of state function,

$$\boldsymbol{x}(k+1) = \boldsymbol{A}_\phi \boldsymbol{x}(k) + \boldsymbol{A}^{-1}(\boldsymbol{A}_\phi - \boldsymbol{I})\boldsymbol{Bu}(k) + \boldsymbol{A}^{-1}(\boldsymbol{A}_\phi - \boldsymbol{I})\boldsymbol{d}(k) \tag{5}$$

Where,

$$\boldsymbol{A}_\phi = e^{\boldsymbol{AT}} = e^{-\frac{R}{L}T}\begin{bmatrix} \cos\omega_e T & \sin\omega_e T \\ -\sin\omega_e T & \cos\omega_e T \end{bmatrix}, \quad \boldsymbol{I} = \begin{bmatrix} 1 & 0 \\ 0 & 1 \end{bmatrix}$$

When the sampling period T is small enough, having the following approximation, $\cos\omega_e T \approx 1$, $\sin\omega_e T \approx \omega_e T$, $e^{-\frac{R}{L}T} \approx 1 - \frac{R}{L}T$。 As a result, the parameter matrices in (5) can be simplified as follows,

$$\boldsymbol{A}_\phi \approx \begin{bmatrix} 1-\frac{R}{L}T & \omega_e T \\ -\omega_e T & 1-\frac{R}{L}T \end{bmatrix}, \quad \boldsymbol{A}_\phi - \boldsymbol{I} \approx \boldsymbol{AT}$$

At last, discrete current predictive model of PMSM is shown as follows,

$$\boldsymbol{x}(k+1) = \boldsymbol{F}(k)\cdot\boldsymbol{x}(k) + \boldsymbol{Gu}(k) + \boldsymbol{H}(k) \tag{6}$$

Where,

$$\boldsymbol{x}(k) = [i_d(k) \quad i_q(k)]^T, \quad \boldsymbol{u}(k) = [u_d(k) \quad u_q(k)]^T,$$

$$\boldsymbol{F}(k) = \begin{bmatrix} 1-\frac{TR}{L} & T\omega_e(k) \\ -T\omega_e(k) & 1-\frac{TR}{L} \end{bmatrix}, \quad \boldsymbol{G} = \begin{bmatrix} \frac{T}{L} & 0 \\ 0 & \frac{T}{L} \end{bmatrix},$$

$$\boldsymbol{H}(k) = \begin{bmatrix} 0 \\ -\frac{T\psi_f}{L}\omega_e(k) \end{bmatrix}。$$

B. Space Vector Modulation (SVPWM)

Voltage source inverter (VSI) is a translator which codes the analog voltage into digital signals and output the signals to load. Essentially VSI is a discrete quantized system. Fig 1 is the structure of 3 phases VSI. The switch states are complementary of two IGBTs for each arm, so the inverter has 8 different switch states in number.

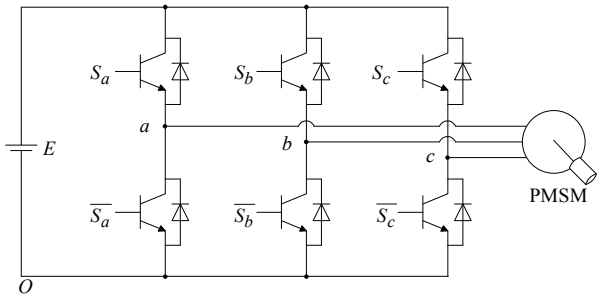

Figure 1. Structure of three phase voltage source inverter

TABLE I. SWITCH STATE OF VSI

No.	0	1	2	3	4	5	6	7
S_a	0	0	0	0	1	1	1	1

S_b	0	0	1	1	0	0	1	1
S_c	0	1	0	1	0	1	0	1

The 8 space voltage vectors of 3 phases VSI is shown in Fig 2, where the amplitude of 6 active voltage vectors is 2*E*/3. The active voltage vectors form a regular hexagon in space, and split the vector space into 6 sections, moreover $\vec{V}_{0,7}$ is zero voltage vectors. Reference voltage vector $\vec{u}_s$ can be calculated from voltage commands u^*_d, u^*_q and rotor angle θ.

The relationship of reference voltage vector $\vec{u}_s$ and basic voltage vectors of VSI is shown in Fig 3. The action time of basic voltage vectors can be calculated from (7).

$$\begin{cases} t_a V_a + t_b V_b = u_s T \\ t_0 = T - t_a - t_b \end{cases} \tag{7}$$

Where, V_a,V_b are the basic voltage vectors which are adjacent to the reference voltage vector $\vec{u}_s$. t_a,t_b,t_0 are the action time of basic voltage vectors V_a,V_b and V_0 respectively, they can expressed as (8).

$$\begin{cases} t_a = \dfrac{\sqrt{3}}{2}(-\sqrt{3}\sin(\theta-\gamma)-\cos(\theta-\gamma))\dfrac{u_s}{E}T \\ t_b = \sqrt{3}\cos(\theta-\gamma)\dfrac{u_s}{E}T \end{cases} \tag{8}$$

Where, $\gamma = \arctan^{-1}(u^*_d / u^*_q)$.

PWM strategy is the most important part of current regulation, and it can be categorized into 3 parts: sinusoidal PWM, space vector PWM, optimal PWM. Space vector PWM is more suitable to instantaneous current control for the advantages of large range of linearity control, low harmonics and fast transient response. The current controller outputs d-q axis voltage commands, and translate the commands into switch signals through SVPWM strategy.

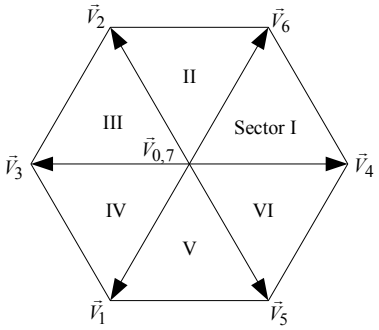

Figure 2. Basic voltage vectors of three phase VSI

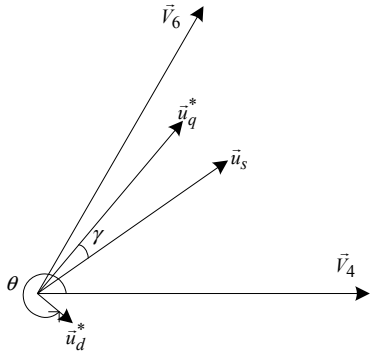

Figure 3. Relation of reference voltage vector and basic voltage vector of VSI

III. PREDICTIVE CURRENT CONTROL ALGORITHM

A. Model of current controller

The structure of predictive control algorithm that proposed in this paper is shown in Fig 4.

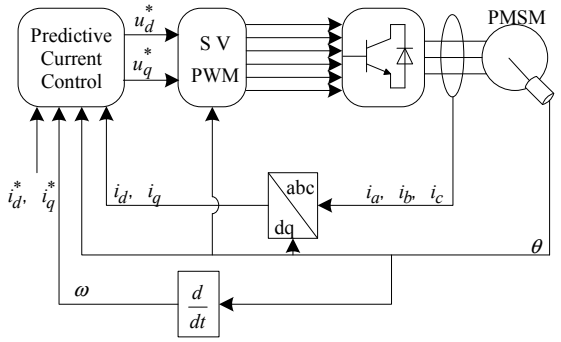

Figure 4. Block diagram of predictive current control

According to the predictive current model (6), letting the current commands as the predictive value of next period, then the formula of *d-q* axis voltage can be got as (9).

$$\begin{bmatrix} \overline{u_d(k)} \\ \overline{u_q(k)} \end{bmatrix} = \boldsymbol{G}^{-1}\left\{ \begin{bmatrix} i^*_d(k) \\ i^*_q(k) \end{bmatrix} - \boldsymbol{F}(k)\begin{bmatrix} i_d(k) \\ i_q(k) \end{bmatrix} - \boldsymbol{H}(k) \right\} \tag{9}$$

B. Robust current control

Quadrature axis predictive current formula can be extracted from the predictive current model (6), that is shown below.

$$u_q(k) = (R - \frac{L}{T})i_q(k) + \frac{L}{T}i_q(k+1) + L\omega_e(k)\cdot i_d(k) + T\psi_f\omega_e(k) \tag{10}$$

Ideal parameters of the motor are need to predict the motor currents in the proposed algorithm, then generates the voltage commands to force motor currents varying with relevant

references. The voltage command of q axis can be calculated from (11), where subscript "$_0$" represent the parameters which used in predictive algorithm, and superscript "*" represent the reference value of relevant variables.

$$u_q^*(k) = (R_0 - \frac{L_0}{T})i_q(k) + \frac{L_0}{T}i_q^*(k+1) + L_0\omega_e(k)\cdot i_d(k) + T\psi_{f0}\omega_e(k) \quad (11)$$

[16,17] say the primary factor of system stabilization is the motor inductance deviation. As for the mismatch of resistance and flux, they have small impact on the system stabilization. If the actual inductance value is smaller than a half of the inductance value used in control algorithm that will lead to system divergence. In order to overcome the drawback, a modified robust current control algorithm is adopted. Introducing two weight factors α, β and $\alpha + \beta = 1$, the predictive equation can be re-written as (12), where $\hat{i}_{d,q}(k)$ represent predictive d-q axis motor current in the kth control period, i.e. $\hat{i}_{d,q}(k) = i_{d,q}^*(k)$.

$$u_q^*(k) = (R_0 - \frac{L_0}{T})[\alpha\hat{i}_q(k) + \beta i_q(k)] + \frac{L_0}{T}i_q^*(k+1) + L_0\omega_e(k)\cdot[\alpha\hat{i}_d(k) + \beta i_d(k)] + T\psi_{f0}\omega_e(k) \quad (12)$$

When the parameters used in the control algorithm are mismatched with the actual values, actual current $i_q(k+1)$ is not equal to its reference value $i_q^*(k+1)$, letting $u_q^*(k)$ in (12) equals to $u_q(k)$ in (10), then the relationship between actual current value and its reference can be got as (13).

$$\begin{aligned} &Li_q(k+1) + [(RT - L) - (R_0T - L_0)\beta]i_q(k) \\ &= (R_0T - L_0)\alpha i_q^*(k) + L_0 i_q^*(k+1) + \\ &\quad TL_0\omega_e(k)\cdot[\alpha i_d^*(k) + \beta i_d(k)] - \\ &\quad TL\omega_e(k)\cdot i_d(k) + T^2(\psi_{f0} - \psi_f)\cdot\omega_e(k) \end{aligned} \quad (13)$$

Treating the back EMF as a perturbation in the current loop, when the sampling period T is small enough and applying $i_d = 0$ control strategy, (13) can be simplified as (14). (15) is the discrete transfer function of (14). The robust predictive current control model is shown in Fig 5.

$$\begin{aligned} &Li_q(k+1) + (\beta L_0 - L)\cdot i_q(k) \\ &\quad = -\alpha L_0 i_q^*(k) + L_0 i_q^*(k+1) \end{aligned} \quad (14)$$

$$\frac{i_q(z)}{i_q^*(z)} = \frac{L - z^{-1}\alpha L_0}{L - z^{-1}(L - \beta L_0)} \quad (15)$$

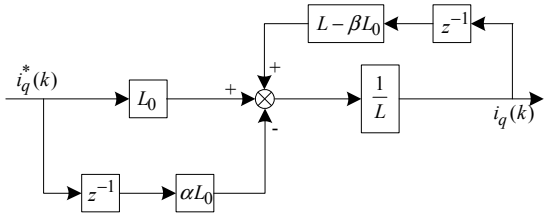

Figure 5. Robust current control model

Considering the influence of poles in discrete domain to the system stabilization, if $L_0 / L < 2/\beta$ that means the system is stable. Because of β<1, along with β decreasing the allowable inductance error is increasing. Fig 6 shows the relationship of poles P_z and β, L_0/L, it can be found that the proposed algorithm make the system still stable when the inductance error is large.

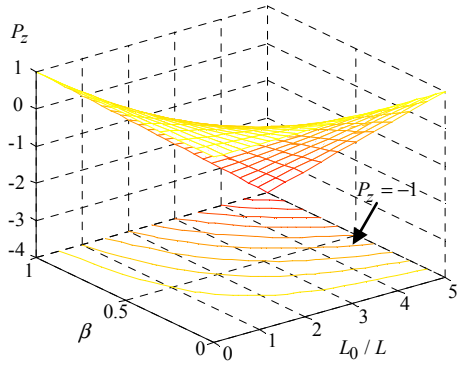

Figure 6. Relationship of poles P_z and β, L_0/L

C. *Voltage restriction*

It can not output overlarge voltage in practical system, thus the command voltages which calculated from predictive model have to be restricted. On the basis of amplitude coordinate transformation the maximum output voltage in the synchronous rotating coordinate is $2/3E$, where E is the DC bus voltage. After the voltage commands calculated through (9), adopting (16) to restrict the actually output voltages.

$$if\left(\sqrt{u_d^2 + u_q^2} > 2E/3\right) \Rightarrow \begin{cases} u_d^* = \dfrac{2E/3}{\sqrt{u_d^2 + u_q^2}}u_d \\ u_q^* = \dfrac{2E/3}{\sqrt{u_d^2 + u_q^2}}u_q \end{cases} \quad (16)$$

IV. SIMULATION AND EXPERIMENT

In this section the simulation and experimental waveforms of the proposed predictive current algorithm will be shown. Motor parameters both in simulation and experiment are: rated power 750W, rated speed 3000 r/min, stator resistance 0.45Ω,

inductance L_d=L_q=3.9×10^{-3}H, poles 4, inertial 8.53×10^{-5} kg·m^2, the incremental encoder is 2500 p/rev. Simulation environment is based on matlab/simulink, and the practical experiment platform is based on TMS320F2812. The current control frequency both in simulation and practical experimental is 10 kHz. In practical experiment the speed loop applies a PI controller, and the parameters of PI regulation in all of the experiments are the same, to evaluate the performance of difference current control strategy.

Fig 7 is the simulation waveform of quadrature and direct axis currents with inductance error, the simulation condition is 3000 r/min step start without load. Where in (a) β=1, L_0/L=3, in (b) β=0.5, L_0/L=3. It can be found that the motor currents have significant oscillation when L_0/L=3. However if tuning β to 0.5, the oscillation disappeared and the control system still stable.

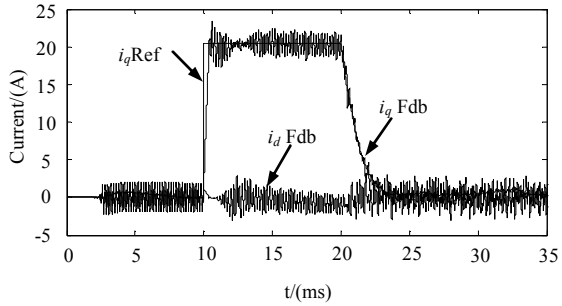

(a) β=1，L_0/L=3

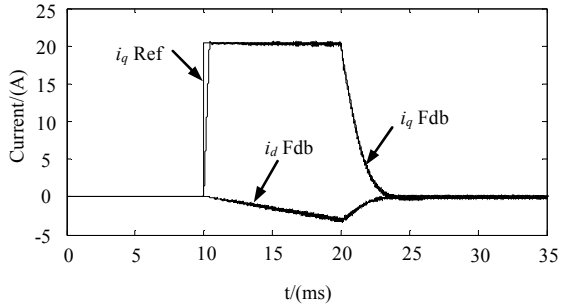

(b) β=0.5，L_0/L=3

Figure 7. *d-q* axis current with model parameter error

Fig 8 is the simulation waveform of predictive current control system response. It can be found that, the motor currents trace the relevant reference perfectly no matter during the transient of 3000 r/min step start or step nominal load. It indicates that the proposed predictive algorithm has the ideal control effect during both the dynamic and static process.

Fig 9 is the experiment result of 3000 r/min step start without load. The motor speed and *q* axis current component are output by DAC model. It has the same results compared with Fig 8.

Fig 10 the waveform of phase current and DC bus voltage working at 3000 r/min speed command no load with large load inertial. Where in (a) the current control system adopts the traditional PI controller, in (b) the system adopts the proposed predictive current control algorithm, and the speed loop in both (a) and (b) adopt the same PI controller. It can be seen from (a) that current and DC bus voltage have significant oscillation caused by speed oscillation. Therefore if the speed loop PI controller has the same parameters, the predictive current control not only improves the response of current loop but also improves the speed loop performance. Compared with (a) and (b) during transient of constant accelerating process amplitude control of predictive algorithm is superior than the traditional FOC, especially at the first peak of phase current.

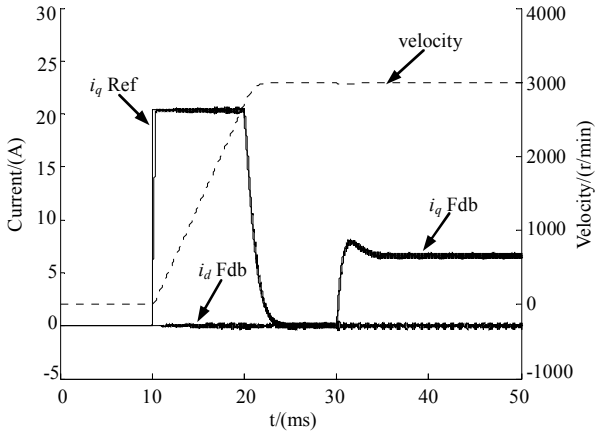

Figure 8. The waveform of system response during transient

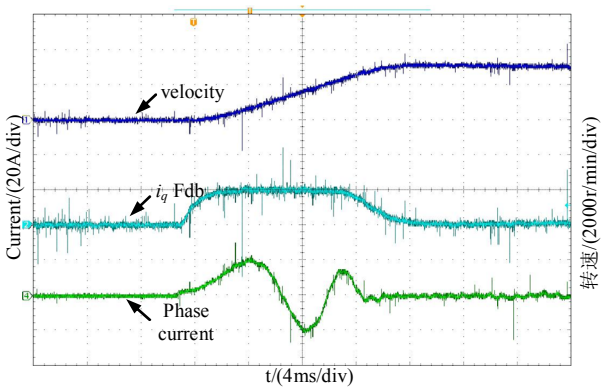

Figure 9. The experimental waveform of system response during transient

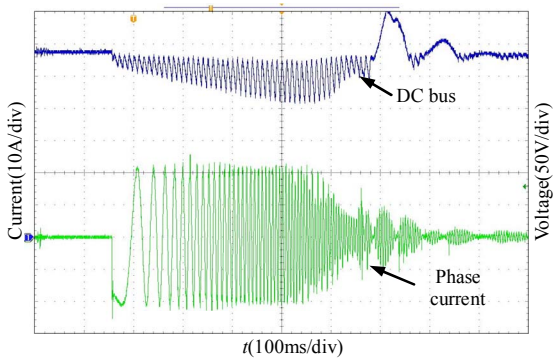

(a) traditional PI controller

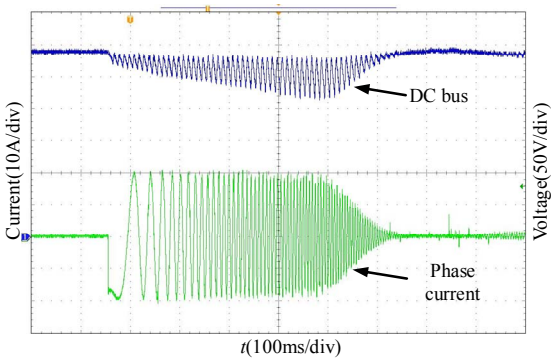

(b) proposed predictive controller

Figure 10. VoltageDC-BUS and phase current waveform

V. CONCLUSION

Based on the principle of deadbeat control, this paper proposed a predictive current control using PMSM mathematical model in synchronous rotating coordinate. This paper also proposed a robust current control algorithm to improve the system stabilization when there have parameter errors in system model, especially for the inductance. Simulation and experiment are to verify the performance of proposed current control algorithm, the results show that the predictive current control algorithm makes the motor current tracing their reference more accurately compared with traditional FOC, and without losing the stabilization.

REFERENCES

[1] Casadei D, Profumo F, Serra G, Tani A. FOC and DTC: two viable schemes for induction motors torque control[J]. IEEE Transactions on Power Electronics, 2002, 17(5): 779-787.

[2] Serrano-Iribarnegaray L, Martinez-Roman J. A Unified Approach to the Very Fast Torque Control Methods for DC and AC Machines [J]. IEEE Transactions on Industrial Electronics, 2007, 54(4): 2047-2056

[3] Wang Hong, Yu Yong, Xu Dianguo. The position servo system of PMSM[J]. Proceedings of the CSEE, 2004, 24(7): 151-155.

[4] Jia Wu, Dongsheng Zhang, Yongdong Li. Fully digital implementation of PMSM servo based on a novel current control strategy[C]. Proceedings of the Power Conversion Conference, Nagaoka, 1997, 1: 133-138.

[5] ENG Li, ZHANG Kai, KANG Yong, CHEN Jian. Performance Analysis and Improvement of Digital Controlled PWM Inverter[J]. Proceedings of the CSEE, 2006, 26(18): 65-70.

[6] CAI Huabin, XIAO Jian, YAN Shu. Multirate Direct Torque Control Based on DSP[J]. Proceedings of the CSEE, 2008, 28(27): 114-119.

[7] Griva G, Ilas C, Eastham J F, Profumo F, Vranka P. High performance sensorless control of induction motor drives for industry applications[C]. Proceedings of the Power Conversion Conference, Nagaoka, Japan, 1997, 2: 535-539.

[8] WANG Hongjia, YANG Ming, NIU Li, XU Dianguo. Current Loop Bandwidth Expansion for Permanent Magnet AC Servo System[J]. Proceedings of the CSEE, 2010, 30(12): 56-62.

[9] Cortes P, Kazmierkowski M P, Kennel R M, Quevedo D E, Rodriguez J. Predictive Control in Power Electronics and Drives[J]. IEEE Transactions on Industrial Electronics, 2008, 55(12): 4312-4324

[10] Xuefang LinShi, Morel F, Llor A M, Allard B, Retif J,M. Implementation of Hybrid Control for Motor Drives[J]. IEEE Transactions on Industrial Electronics, 2007, 54(4): 1946-1952.

[11] Morel F, Xuefang Lin-Shi, Retif J M, Allard B, Buttay C. A Comparative Study of Predictive Current Control Schemes for a Permanent-Magnet Synchronous Machine Drive[J], IEEE Transactions on Industrial Electronics, 2009, 56(7): 2715-2728.

[12] Pacas M, Weber J. Predictive direct torque control for the PM synchronous machine[J]. IEEE Transactions on Industrial Electronics, 2005, 52(5): 1350-1356.

[13] Morales R, Pacas M. A Predictive Torque Control for the Synchronous Reluctance Machine Taking Into Account the Magnetic Cross Saturation[J], IEEE Transactions on Industrial Electronics, 2007, 54(2): 1161-1167.

[14] Abu-Rub H, Guzinski J, Krzeminski Z, Toliyat H A. Predictive current control of voltage-source inverters[J]. IEEE Transactions on Industrial Electronics, 2004, 51(3): 585-593.

[15] Gatto G, Marongiu I, Serpi A, Perfetto A. Predictive Control of Synchronous Reluctance Motor Drive[C]. IEEE International Symposium on Industrial Electronics, Vigo, Spain, 2007, 1: 1147-1152.

[16] Morel F, Xuefang L-S; Retif J-M, Allard B, Buttay C. A Comparative Study of Predictive Current Control Schemes for a Permanent-Magnet Synchronous Machine Drive[J]. IEEE Transactions on Industrial Electronics, 2009, 56(7): 2715-2728.

[17] Moreno J C, Huerta J M E, Gil R G, Gonzalez S A. A Robust Predictive Current Control for Three-Phase Grid-Connected Inverters[J]. IEEE Transactions on Industrial Electronics, 2009, 56(6): 1993-2004.